Frequency Prediction of Synchronous Generators in a Multi-machine Power System with a Photovoltaic Plant Using a Cellular Computational Network

Yawei Wei, *Student Member IEEE*, Iroshani Jayawardene, *Student Member IEEE*,
Ganesh Kumar Venayagamoorthy, *Senior Member, IEEE*
Real-Time Power and Intelligent Systems Laboratory,
Holcombe Department of Electrical and Computer Engineering,
Clemson University, Clemson, SC, USA
yaweiw@clemson.edu, rjayawa@clemson.edu, gkumar@ieee.org

***Abstract*—Conventional power systems with photovoltaic (PV) plants experience frequency and power fluctuations due to high variability of PV power. Automatic generation control is implemented to control power outputs of generators and stabilize the system frequency. It is desirable with increasing levels of PV penetration to have the foresight of frequency fluctuations to enable advanced controls. A new methodology is presented in this paper for predicting frequency of synchronous generators in a power system with solar PV. A cellular computational network (CCN) is used to perform multi-timescale frequency prediction. CCNs are scalable and distributed computing paradigms. Thus, CCNs are suitable for fast prediction of frequency of synchronous generators distributed spatially across a power system. The inputs to cells of CCN are derived from phasor measurement unit (PMU) measurements of frequency and voltage phasor at the respective generator buses. Past and current measurements enable multi-timescale frequency predictions of synchronous generators. Typical multi-timescale frequency predictions using the CCN are illustrated on a two-area four-machine power system with solar PV integrated.**

I. INTRODUCTION

Power systems integrated with solar photovoltaic (PV) plants becomes an inevitable trend for next few decades, as PV could be an important solution for decentralized load or remote customers in many situations [1]. However, the power fluctuations of PV systems caused by weather changes and variability of solar irradiation requires modernization and innovation of the conventional power systems. Furthermore, rural electrification and expansion of the grid requires distributed generation such as PV [2], [3]. Power fluctuation results in frequency fluctuation and thus, frequency measurements are good indicators and feedback signals to mitigate power fluctuations through suitable governor controls such as automatic generation control (AGC). In traditional generator-turbine systems, frequency could be estimated or predicted considering the time-delayed turbine-generator response through perturbation analysis [4], [5]. However, with a continuous increasing rate of PV power penetration, power system frequency estimation with historical data is not enough for mitigating power fluctuations. Today, many bulk power systems have deployed significant number of phasor measurement units (PMUs) and enable fast monitoring of grid conditions [1], [6]. PMUs produce a significant amount of data over a short period time given their sampling rates of 30Hz/25 Hz, depending on the location of a power system.

Several power frequency estimation/prediction algorithms have been presented to address this challenge. A hybrid method consisting of Taylors expansion and Fourier algorithm was proposed for frequency estimation in [5]. It performs well for different sampling rate sensors and compensates the error in a historical data, but is not suitable for real-time monitoring with the significant amount of PV power fluctuations.

Refs. [7]–[9] have discussed computational intelligence approaches including support vector machines and neural networks for frequency predictions arising from the integration of renewable energy sources as wind power. Their results show good performances for wind integrated system with single time interval frequency prediction, however prediction time interval is longer.

Although different methods for estimating, utilizing or even early prediction frequency have been discussed in previous studies, the scalability and accuracy for multi-machine power system with solar PV integration remain challenges. Refs. [10], [11] have introduced a cellular neural network approach to provide a scalable system-wide prediction framework, also referred to as the cellular computational network (CCN) [12]. The CCN framework allows for the use of distributed computing to provide situational intelligence for grid operations [13]. Ref. [14] has introduced the initial cellular neural network structure for empowering circuit distributed analysis.

In this paper, a cellular computational network is used to perform the frequency prediction over a multi-timescale. The

The funding provided by National Science Foundation,USA under grant IIP #1312260 and ECCS #1408141 are acknowledged.

978-1-4799-7560-0/15 $31.00 © 2015 IEEE
DOI 10.1109/SSCI.2015.103

inputs to cells of the CCN are derived from PMU measurements of frequency and voltage phasors at the respective generator buses. Past and current measurements enable multi-timescale predictions of synchronous generator frequencies. Typical multi-timescale frequency predictions using a CCN are illustrated on a two-area four machine power system with solar PV integrated.

The rest of the paper is organized as following: Section II provides an overview of the CCN structure for a two-area four-machine power system with solar PV. Section III describes a CCN based multi-timescale prediction framework and algorithm. Simulation results obtained with a CCN under laboratory, and actual weather conditions are provided in Section IV. Finally, Section V provides some conclusions and future work from the study performed in this paper.

II. CCN ARCHITECTURE

Cellular computational network (CCN) is a distributed and scalable architecture which uses the concept of cells to model a complex system. Generally, a cell is configured to learn or compute the required output based on some computing algorithm and utilizing the available information at its input(s). The inputs could be external, from the cell's past output(s) and/or the adjacent cells' past outputs. The computing algorithm could be empowered with capabilities to enhance its functionality. The connections between the cells are driven by the topology of the complex network being mapped or modeled. Through the cellular connections the system-wide dynamics is propagated to the respective cells over time. Neighboring cells communicate/relate with each other faster (and directly) than cells farther away. Because of these unique advantages, the CCN architecture becomes suitable for modeling power system dynamics, especially the interactions of synchronous generators with variable generation sources.

CCN in this study is implemented to predict the generator frequency of a two-area four-machine PV integrated power system. Each generator of the power system is considered as a cell. Cells can communicate with their neighboring cells to predict the frequencies of the generators in the system.

Fig. 1 shows a CCN implementation for frequency prediction on a two-area-four-machine power system. Generators G1, G2, G3 and G4 are connected to bus lines 1, 2, 3 and 4 respectively. A 200 MW PV plant is integrated to area 2. The entire system is modeled on a real time digital simulator (RTDS). Real-time weather information captured at Clemson University's Real-Time Power Intelligent Systems Laboratory is used to drive the PV plant. Two automatic generation controls (AGCs) are implemented, one in each area of the power system, to maintain the desired system frequency. The AGC controller in area 2 with PV power is presented in Fig. 2. A multi-layer perception (MLP) neural network is used as the computational unit of each cell in the CCN implementation. Each MLP is trained using data obtained from simulated PMUs on the power system. The CCN framework allows each generator to determine its near

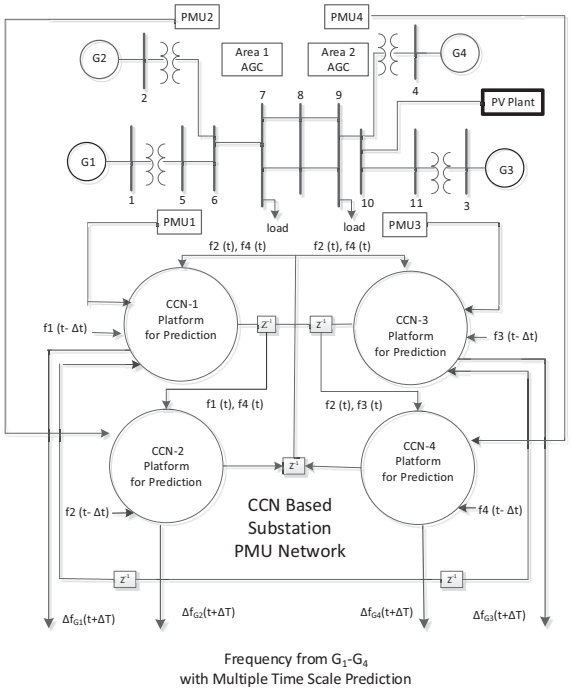

Fig. 1. CCN based multi-timescale frequency predictions for a two-area four-machine PV system.

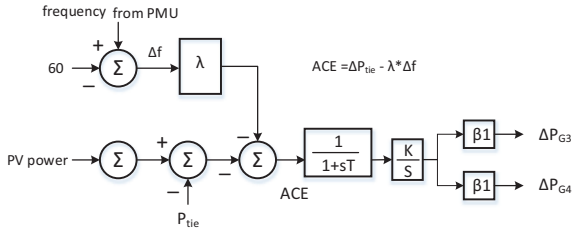

Fig. 2. Automatic generation control in area 2.

future frequency state independently and simultaneously. In general, for a ΔT time ahead forecasting, $(t + \Delta T)$, the frequency prediction function can be expressed as,

$$\hat{f}_i(t+\Delta T) = F\Big\{ f_i(t),\ \Delta V_{ref_i},\ f_i(t-\Delta T),\ f_i(t-2\Delta T),\ \hat{f}_j(t),\ \hat{f}_k(t)\Big\},\quad i = 1\ to\ 4 \tag{1}$$

where $\hat{f}_i(t+\Delta T)$ is predicted ΔT time ahead frequency for i_{th} generator; ΔV_{ref_i} represents the reference voltage of each generator in the system of Fig. 1; $f_i(t-\Delta T)$ refers to the frequency at the previous time step and $\hat{f}_j(t)$, $\hat{f}_k(t)$ represent the frequency of the neighboring generators at time t. The PV system is treated as a perturbation agent to the rest of the system. Its power output varies over time and cannot be controlled since the maximum power utilization is desirable.

III. CCN BASED FREQUENCY PREDICTION

A general process of CCN based multi-timescale frequency prediction could be summarized as shown in Fig. 3. Real-time data from power system (PMU measurements of generator and PV outputs) are inputs into CCN prediction platform for multiple time-interval predictions (from t to $t + \Delta T$). Based on (1), the all four generator's frequency prediction in the two-area four-machine system is implemented as shown in (2) to (5) below.

$$\hat{f}_1(t+\Delta T) = F\Big\{ f_1(t),\ \Delta V_{ref_1}(t),\ f_1(t-\Delta T),\ f_1(t-2\Delta T),\ \hat{f}_2(t),\ \hat{f}_4(t)\Big\} \quad (2)$$

$$\hat{f}_2(t+\Delta T) = F\Big\{ f_2(t),\ \Delta V_{ref_2}(t),\ f_2(t-\Delta T),\ f_2(t-2\Delta T),\ \hat{f}_1(t),\ \hat{f}_3(t)\Big\} \quad (3)$$

$$\hat{f}_3(t+\Delta T) = F\Big\{ f_3(t),\ \Delta V_{ref_3}(t),\ f_3(t-\Delta T),\ f_3(t-2\Delta T),\ \hat{f}_2(t),\ \hat{f}_4(t)\Big\} \quad (4)$$

$$\hat{f}_4(t+\Delta T) = F\Big\{ f_4(t),\ \Delta V_{ref_4}(t),\ f_4(t-\Delta T),\ f_4(t-2\Delta T),\ \hat{f}_3(t),\ \hat{f}_1(t)\Big\} \quad (5)$$

The APE and MAPE are commonly used for prediction performance evaluation [10]. To evaluate the CCN's frequency prediction performance, absolute percentage error (APE) and mean absolute percentage error (MAPE) given in (6) and (7), respectively are computed over a period of time.

$$APE = \Big|\frac{A_t - P_t}{A_t}\Big| \times 100\% \quad (6)$$

$$MAPE = \frac{1}{n}\sum_{t=1}^{n}\Big|\frac{A_t - P_t}{A_t}\Big| \times 100\% \quad (7)$$

where A_t and P_t are corresponding actual and predicted values and n is the number of sampled data in a certain time period.

IV. RESULTS AND DISCUSSIONS

In this study, the two-area four-machine power system is considered under three PV power output average conditions, namely high level (above 140 MW), moderate level (between 70 MW and 140 MW) and low level (below 70 MW).

For this study, the PMU measurements are used by CCN in the frequency prediction process as shown in Fig. 3. The PMU data are generated by RTDS for power system inc. consideration (Fig. 1). The solar irradiance for PV power gradually increases and reaches around its peak around noon on a normal day. In order to reflect small frequency fluctuations in PV integrated power system, a pseudo-random binary signal (PRBS), as shown in Fig. 4, has been applied to the generator excitation systems of G1 and G2 in area 1. Frequency predictions of the four generators under PRBS signal conditions are shown in Fig. 5. In this study, a ten-minute data segment has been collected for every condition for CCN learning. These figures represent

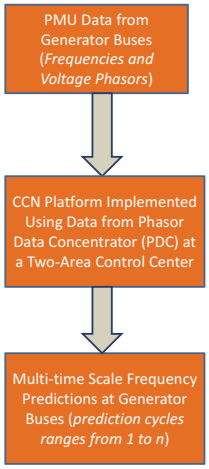

Fig. 3. CCN based multi-timescale frequency predictions implementation flow diagram.

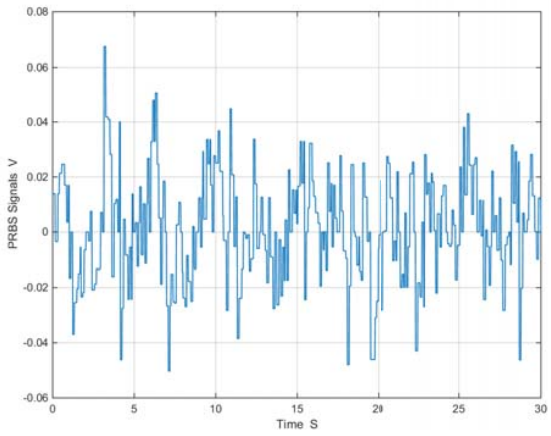

Fig. 4. PRBS signals applied to generate system-wide fluctuations.

presented below for generator frequency predictions are for a thirty-second period. The predictions for one cycle ($16ms$) ahead are shown in Fig. 5. Table. I shows the performance of the prediction results. The largest errors normally occur at peak points, especially for rapid frequency jumps, up or down. Among all four generators, it is observed for the system in Fig. 1 the frequency prediction of generator G2 has relatively larger prediction errors than the others in Table. I.

Six different time scale predictions are performed at time t, namely $t + 16\ ms$, $t + 100\ ms$, $t + 200\ ms$, $t + 300\ ms$, $t + 400\ ms$ and $t + 500\ ms$, as to 1, 6, 13, 19, 25, 31 cycles ahead, respectively. Since it is observed G2 has the largest prediction error (APE and MAPE), predicted frequencies of G2 are shown for multiple timescales under the three different PV power output conditions below.

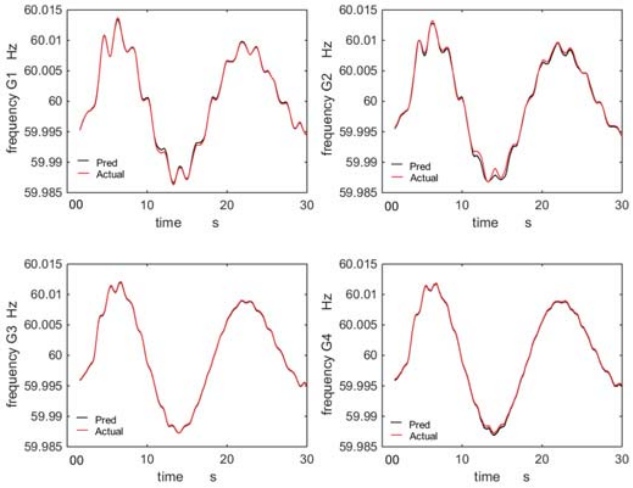

Fig. 5. Frequency predictions with PRBS signals in Fig. 4

TABLE I
MAXIMUM APES AND MAPES OBTAINED FOR FREQUENCY PREDICTIONS WITH PRBS SIGNALS

Generator Index.	maximum APE value (%)	MAPE value (%)
G1	0.016	0.014
G2	0.02	0.019
G3	0.016	0.014
G4	0.016	0.013

The system is simulated with Clemson, SC sunny, moderate and cloudy solar irradiance conditions from 00:00:00 to 23:59:59 with one second sampling size. Fig. 6 shows three weather conditions, namely sunny day (September 14, 2013), moderate day (September 16, 2013) and cloudy day (September 21, 2013), used in this study.

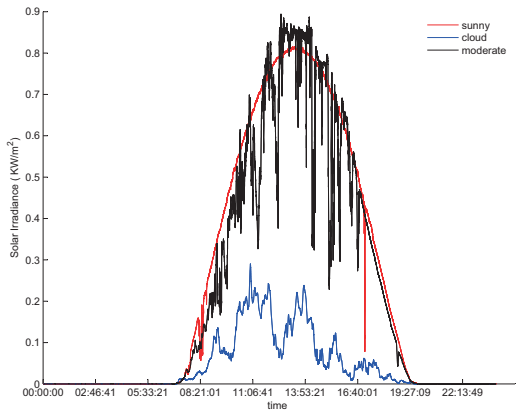

Fig. 6. Solar irradiance variations under sunny, moderate and cloudy weather conditions obtained at the RTPIS Lab in Clemson, SC.

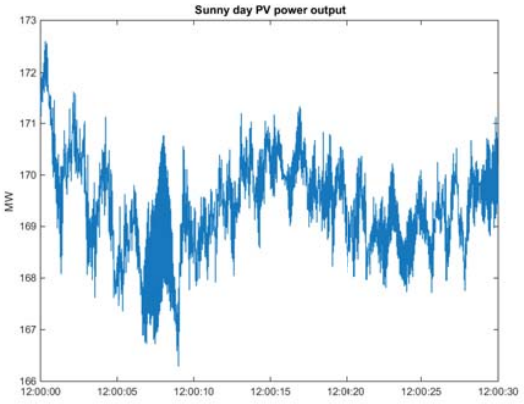

Fig. 7. PV power output from 12:00:00 to 12:00:30 pm on a sunny day.

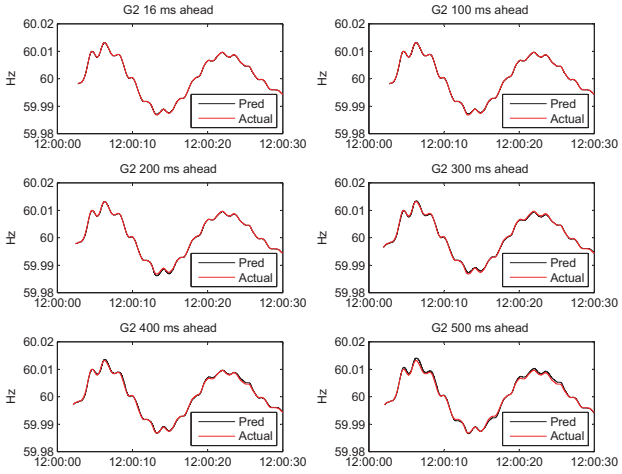

Fig. 8. Multi-timescale frequency predictions for G2 under high PV power output condition.

A. Multi-timescale Frequency Predictions During High PV System Power Outputs

PV power output for thirty seconds from 12:00:00 pm to 12:00:30 pm on a sunny day (Fig. 6) is shown in Fig. 7. Based on the PV power output curve, it is clear that the PV power fluctuates between 166 MW and 173 MW. Frequency predictions for G2 for multiple time steps under such PV power output conditions are shown in Fig. 8. The maximum APE and corresponding MAPE values are shown in Table. II. The multi-timescale predictions results show that 1 cycle and 6 cycles predictions are more accurate than 13 to 31 cycles ahead predictions. The 31 cycles (517 ms) prediction value shows a relative larger maximum APE value of 0.25%, and a MAPE value of 0.194%.

B. Multi-timescale Frequency Predictions During Moderate PV System Power Outputs

In this case, a moderate day in Fig. 6 is used to simulate the PV power. The PV power output obtained from 16:00:00

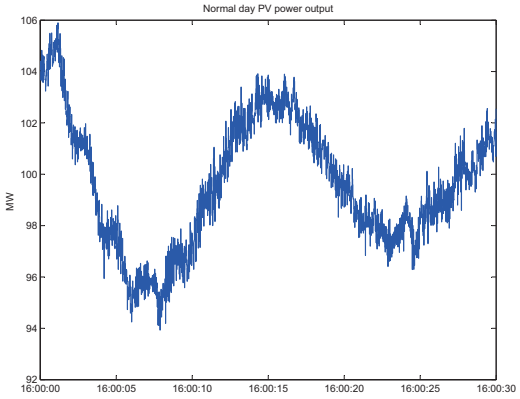

Fig. 9. PV power output from 16:00:00 to 16:00:30 on a moderate day.

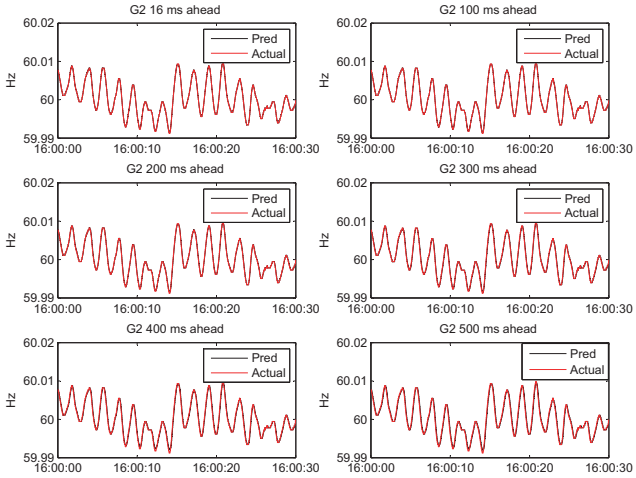

Fig. 10. Multi-timescale frequency predictions for G2 during a moderate PV power output condition.

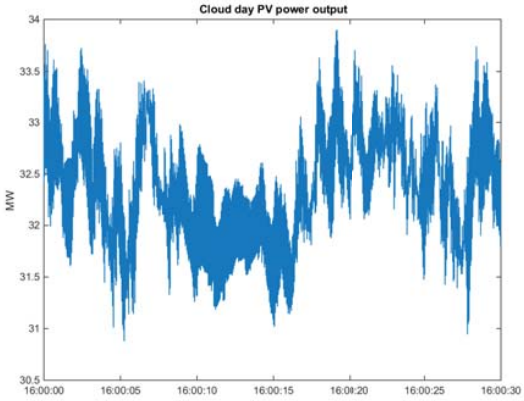

Fig. 11. PV power output from 16:00:00 to 16:00:30 on a cloudy day

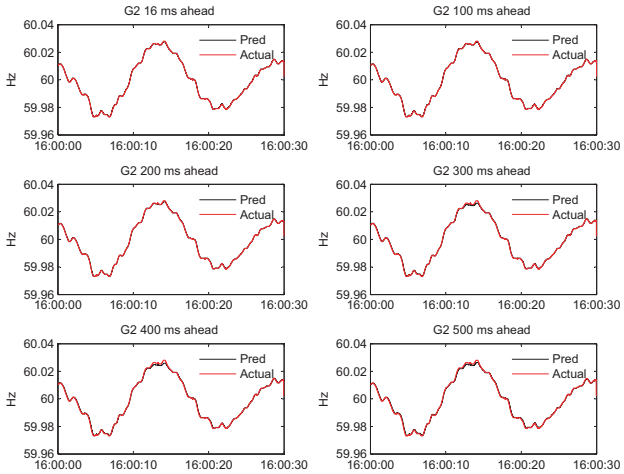

Fig. 12. Multiple time scale frequency predictions for G2 under low PV power condition.

to 16:00:30 is shown Fig. 9 to vary in the range of 93MW to 106MW. Multi-timescale frequency predictions of G2 during a moderate PV power integration are given in Fig. 10. These maximum APE and MAPEs are summarized in Table.II.

According to the Fig. 10 and Table. II, it is clear that the frequency has been perturbed severely under a moderate PV power output condition. Moreover, these fluctuations at half PV power output level (100MW) give a larger system error than other cases, which leads to large maximum APE and MAPE values of 0.23% and 0.193%, respectively.

C. Multi-timescale Frequency Predictions During Low PV System Power Outputs

PV output power simulated on a cloudy day (in Fig. 6) is used in this case study. Fig. 11 shows the PV power variation from 16:00:00 to 16:00:30 in the range of 30MW to 34MW. Multi-timescale predictions of generator G2's frequency, 1 cycle to 31 cycles ahead, under PV power conditions shown in the Fig. 11 are depicted in Fig. 12. Table. II presents the calculated APE and MAPE values. Impact of the frequency swing is not significant under low PV system power output conditions, even with a relative high rate of PV fluctuations, comparing to the last case study. This has led to better prediction results. For the 31 cycles ahead prediction, the APE is 0.2% and the MAPE is 0.16%.

Based on the results obtained, the predictions for longer time intervals (cycles) show more uncertainty. Additionally,

TABLE II
MAXIMUM APES AND MAPES OBTAINED FOR G2 FREQUENCY PREDICTIONS UNDER THREE DIFFERENT PV SYSTEM POWER OUTPUT CONDITIONS AT CLEMSON, SC

t+ΔT time ahead	maximum APE value (%)			MAPE value (%)		
	High	Moderate	Low	High	Moderate	Low
1 cycle	0.016	0.016	0.016	0.0063	0.0045	0.007
6 cycles	0.04	0.03	0.02	0.025	0.021	0.015
13 cycles	0.14	0.08	0.1	0.094	0.063	0.077
19 cycles	0.14	0.133	0.13	0.091	0.086	0.09
25 cycles	0.20	0.16	0.19	0.14	0.105	0.11
31 cycles	0.25	0.23	0.2	0.194	0.193	0.16

large PV plants with different power output conditions have different impacts on system frequency prediction error as expected. The best case is either in constant PV power or low PV power output modes. However, implemented CCN structure predictions have resulted in a sufficient prediction accuracy under all different conditions.

V. CONCLUSION

In this paper, a cellular computational network has been presented for multi-timescale frequency predictions at synchronous generator buses under three typical PV power output conditions. The concept of CCN is illustrated on a two-area four-machine power system. The presented CCN approach is a scalable and distributed approach, applicable to larger and multi-area power systems. According to the accuracy of the results obtained, the CCN based predicted frequencies are applicable in detection of system post-disturbance stability, for development wide area control systems and in the development of countermeasures for cybersecurity attacks.

References

[1] G. K. Venayagamoorthy , I. Jayawardene, *et al.* "Grid Operations with Peneration of Photovoltaic Systems," *2015 Third Southern African Solar Energy Conference,* May 2015.

[2] G. M'boungui,A. A. Jimoh, T. R. Ayodele, "On the adaptation of South Africa experience to combine solar energy and Smart Grid in Namibia," *2013 AFRICON.,* pp.1,5, 9-12, Sept. 2013

[3] P. Zeller and H. M. Libati, "Utilization of solar energy for electrical power supply in rural African areas," *2009 AFRICON.,* pp.1,6, 23-25, Sept. 2009

[4] R. A. Schlueter , G. L. Park and E. Retford, "A Study of Frequency Prediction for Power Systems", *IEEE Trans. on Automatica Control*, vol. AC 23, no. 6, pp.996 -1000, Feb. 1978

[5] R. Jinfeng and M. Kezunovic, "A Hybrid Method for Power System Frequency Estimation," *IEEE Trans. Power Del.*, vol. 27, no. 3, pp.1252-1259, Jul. 2012.

[6] A. G. Phadke and J. S. Thorp, *Synchronized Phasor Measurements and Their Applications,* New York: Springer, 2008.

[7] Q. Bo, "Minimum frequency prediction of power system after disturbance based on the v-support vector regression", in *2014 International POWERCON.*, 2014, pp. 614-619.

[8] S. Kaur and S. Agrawal, "Power Grid Frequency Prediction Using ANN Considering the Stochasticity of Wind Power," in *2013 5th international conf. CICN.*, 2013, pp. 311-315.

[9] L. L. Lai , C. T. Tse , W. L. Chan and A. T. P. So, "Real-time frequency and harmonic evaluation using artificial neural networks", *IEEE Trans. Power Del.*, vol. 14, no. 1, pp.52-59, Jan 1999.

[10] B. Luitel, and G. Venayagamoorthy, "Decentralized Asynchronous Learning in Cellular Neural Networks", in *IEEE Trans. Neural Netw. Learn. Syst.*, vol. 23, no. 11, pp. 1755-1766, Nov. 2012.

[11] L. Grant and G. K. Venayagamoorthy, "Voltage Prediction Using a Cellular Network, in *IEEE PES GM.*, Minneapolis, MN, USA, July 25 - 29, 2010.

[12] B. Luitel, and G. Venayagamoorthy, "Cellular Computational Networks a Scalable Architecture for Learning the Dynamics of Large Networked Systems", in *Neural Networks*, vol. 50, pp. 120-123, Feb. 2014.

[13] G. K. Venayagamoorthy, "Synchrophasor Data Driven Situational Intelligence for Power System Operation *Cigre Grid of the Future Symposium*, Houston, TX, USA, October 20-22, 2014.

[14] L. O. Chua, and L. Yang, "Cellular neural networks: Theory", in *IEEE Trans. Circuits Syst.*, vol. 35, pp. 1257-1272, Oct. 1988.